Computational and Structural Biotechnology Journal 27 (2025) 813–820

Contents lists available at ScienceDirect

Computational and Structural Biotechnology Journal

journal homepage: www.elsevier.com/locate/csbj

Database article

m6A2Circ: A comprehensive database for decoding the regulatory relationship between m6A modification and circular RNA

Yongtian Li [a,b,1], Bianli Gu [c,1], Lixia Ma [c,1], Li-Na He [b,1], Xiaoqiong Bao [b], Yuantai Huang [b], Rui Yang [c], Li Wang [d], Qingtao Yang [e], Haibo Yang [e], Zhixiang Zuo [b], Shegan Gao [c,*], Xueya Zhao [a,*], Ke Chen [f,*]

[a] Department of Hematology, The First Affiliated Hospital of Chongqing Medical University, School of Basic Medical Sciences, Chongqing Medical University, Chongqing 400016, China
[b] State Key Laboratory of Oncology in South China, Cancer Center, Collaborative Innovation Center for Cancer Medicine, Sun Yat-sen University, Guangzhou 510060, China
[c] Henan Key Laboratory of Microbiome and Esophageal Cancer Prevention and Treatment, Henan Key Laboratory of Cancer Epigenetics, Cancer Hospital, The First Affiliated Hospital (College of Clinical Medicine) of Henan University of Science and Technology, Luoyang, China
[d] Department of Hematology, The First Affiliated Hospital of Chongqing Medical, University, Chongqing 400016, China
[e] Information Center of Chongqing Medical University, Chongqing 400016, China
[f] Department of Urology, Tongji Hospital, Tongji Medical College, Huazhong University of Science and Technology, Wuhan 430030, PR China

ARTICLE INFO

Keywords:
N6-methyladenosine
Circular RNA
Database

ABSTRACT

Circular RNA (circRNA) is a class of noncoding RNAs derived from back-splicing of pre-mRNAs. Recent studies have increasingly highlighted the pivotal roles of N6-methyladenosine (m6A) in regulating various aspects of circRNA metabolism, including biogenesis, localization, stability, and translation. Despite the importance of m6A in circRNA metabolism, there remains a substantial gap in comprehensive resources dedicated to exploring m6A modification in circRNA. To bridge this significant gap, we present m6A2Circ (http://m6a2circ.canceromics.org/), a pioneering database designed to systematically explore the regulatory interactions between m6A modification and circRNA. The m6A2Circ database encompasses 198,804 m6A-circRNA associations derived from diverse human and mouse tissues. These associations are meticulously categorized into four levels of evidence supported either by experimental data or by high-throughput sequencing data. Moreover, the database offers extensive annotations, facilitating research into circRNA function and its potential disease implications. Overall, m6A2Circ aims to benefit the research community and bolster novel discoveries in terms of crosstalk between m6A and circRNA.

1. Introduction

Circular RNA (circRNA) is a class of noncoding RNAs generated through the back-splicing of pre-mRNAs. They perform a variety of important functions, including acting as sponges for microRNAs (miRNAs) and RNA-binding proteins (RBPs) [1,2], encoding peptides [3], and regulating transcription [4] and translation [5]. Increasing evidence highlights the pivotal roles that circRNAs play in the onset and progression of various diseases, including but not limited to, cancers [6], reproductive diseases [7], cardiovascular diseases [8], neurological disorders [9] and metabolic diseases [10]. While most research has focused predominantly on m6A modification in mRNA, investigations into m6A modifications in noncoding RNA, particularly circRNA, remain relatively rare. Nonetheless, m6A modification has been reported to facilitate various circRNA-related processes and functions, including their translation [11], degradation [12], and ability to label circRNAs to evade innate immunological surveillance [13]. Notably, m6A-modified circRNAs have been implicated in promoting several types of cancers, such as colorectal [14], cervical [15], and hepatocellular [16] cancers. Recent genome-wide studies have identified widespread m6A modification within circRNA. A comprehensive repository of extensive m6A-modified circRNAs will facilitate the investigation of

* Corresponding authors.
E-mail addresses: gsg112258@haust.edu.cn (S. Gao), 103137@cqmu.edu.cn (X. Zhao), kechen@hust.edu.cn (K. Chen).
[1] The authors wish that, in their opinion, the first four authors should be regarded as joint first authors.

https://doi.org/10.1016/j.csbj.2025.02.018
Received 26 November 2024; Received in revised form 17 February 2025; Accepted 17 February 2025
Available online 21 February 2025

the regulatory role of m6A modification in circRNA; however, such a repository has been lacking.

M6A-seq has been utilized extensively for transcriptome-wide mapping of m6A modifications in linear RNA, including mRNA and long noncoding RNA (lncRNA). Recent studies have developed tools that effectively identify m6A-modified circRNA from m6A-seq data. To date, thousands of m6A-seq datasets have been generated and are available in public databases. The application of these circRNA identification tools to existing datasets will not only create a comprehensive landscape of m6A modification in circRNA but also significantly supplement current circRNA databases, such as circBase [17], circAtlas 3.0 [18], and CIRCpedia v2 [19], which derive circRNA primarily from RNA-seq data.

m6A modification is a dynamic process regulated by "writers," "erasers," and "readers" (collectively known as WERs). Understanding the relationship between circRNA and m6A WERs is crucial for exploring the regulatory roles of m6A modification in circRNA. Reanalyzing public RNA-seq data designed to study the functions of m6A WERs through perturbation techniques can help identify circRNAs regulated by these WERs. Additionally, reanalyzing publicly available RIP-seq data targeting WERs can reveal circRNAs that are potentially bound by these regulators.

In this study, we present m6A2Circ, a user-friendly and comprehensive database dedicated to host m6A-circRNA associations, which aims to elucidate the regulatory relationship between m6A modification and circRNA. Currently, m6A2Circ comprises a total of 198,804 m6A-circRNA associations in humans and mice, derived from published literature and public high-throughput datasets involving various cell lines or tissue types. The m6A-circRNA associations can be classified into two distinct categories: [1] "m6A-modified circRNAs," which are supported by evidence of containing m6A modification sites, and [2] "circRNAs regulated by m6A WERs," referring to those whose biogenesis or functions are modulated by m6A writers, erasers, or readers. There are two evidence levels for this two categories of m6A-cricRNA associations: “Validated m6A-cricRNA associations" that are supported by experimental evidence and “potential m6A-cricRNA associations” that are supported by high-throughput sequencing data (Fig. 1). Moreover, m6A2Circ provides detailed information and functional annotations of circRNAs, including mature sequences, predicted m6A sites, disease associations, miRNA binding sites, RBP binding sites, internal ribosome entry sites (IRESs), and open reading frames (ORFs). Overall, we expect that m6A2Circ will be a valuable resource for researchers aiming to explore the principles of m6A regulation of circRNAs.

2. Materials and methods

2.1. Data collection

A comprehensive systematic review of related literature (Table S1) and high-throughput datasets (Table S2) in m6A2Circ were performed via the National Center for Biotechnology Information (NCBI) PubMed and Gene Expression Omnibus (GEO) databases via the search strategy "(WER gene symbol [All fields]) OR (m6A modification [All fields]) AND (circRNA [All fields])". A total of 175 articles published before May 2023 were meticulously reviewed. These publications employed a variety of experimental methodologies, such as methylated RNA immunoprecipitation quantitative PCR (MeRIP-qPCR), RNA pull-down, RNA immunoprecipitation (RIP), reverse transcription quantitative PCR (RT—qPCR), and Western blotting, to confirm m6A-circRNA associations. Following a rigorous manual curation process, 91 articles providing robust experimental evidence were retained. Detailed information regarding the cell lines, chromosome positions, m6A sites, motifs, affected biological processes, and direct experimental evidence was collected.

To identify potential "m6A-modified circRNAs," we retrieved 200 m6A sequencing (m6A-seq) datasets (100 human and 100 murine) from the publicly accessible Gene Expression Omnibus (GEO) database. To derive potential "circRNAs regulated by m6A WERs" supported by perturbation evidence, we obtained 128 RNA-seq datasets generated under various m6A writer, eraser, or reader (WER) perturbation conditions (e.g., knockout, overexpression) from the GEO database. Additionally, to further supplement the associations between m6A and circRNAs, we collected 44 RNA-binding protein immunoprecipitation sequencing (RIP-seq) datasets that employed antibodies targeting m6A WERs.

The Genome Reference Consortium Human Build 38 (hg38) and Genome Reference Consortium Mouse Build 10 (mm10) were used as the reference genomes for humans and mice, respectively. The gene annotation files “GRCh38.90.chr.gtf” and “GRCm38.94.chr.gtf” were downloaded from Ensembl.

2.2. Derivation of circRNAs regulated by m6A WERs with perturbation evidence from RNA-seq analysis

First, the software fastp [20] was utilized to perform quality control and preprocessing of all RNA-seq raw data. Second, for circRNA identification, two widely recognized tools, CIRI2 [21] and CIRCexplorer2 [22], were employed to detect circRNAs from RNA-seq reads mapped using BWA [23]. Third, the identified circRNAs were subsequently

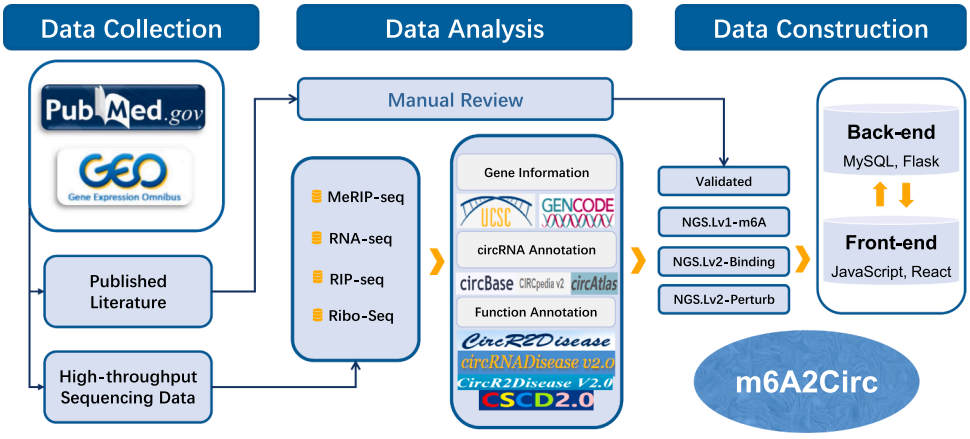

Fig. 1. Overall design and construction of m6A2Circ. The m6A-circRNA associations cataloged in m6A2Circ are categorized into four evidence types: [1] validated—derived from manual curation; [2] NGS.Lv1-m6A—inferred from MeRIP-seq data analysis; [3] NGS.Lv2-Perturb—inferred from m6A WER perturbation followed by RNA-seq and Ribo-seq data analysis; and [4] NGS.Lv2-Bind—inferred from m6A WER RIP-seq data analysis. Additionally, m6A2Circ offers many annotations, including mature sequences, predicted m6A sites, disease associations, miRNA binding sites, RBP binding sites, internal ribosome entry sites (IRESs), and open reading frames (ORFs).

cross-referenced with entries from three publicly available circRNA databases: circBase [17], circAtlas 3.0 [18], and CIRCpedia v2 [19]. Only circRNAs detected by both CIRI2 and CIRCexplorer2, or those identified by one tool and supported by at least one database, were retained for further analysis. Last, the circRNAs were quantified using CIRIquant [25], and deferentially expressed circRNAs were identified via edgeR [26]. The significantly changed circRNAs upon WER perturbation were considered as potential circRNAs regulated by m6A WERs (P value < 0.05, $|\text{fold change}| > 2$).

2.3. Derivation of circRNAs regulated by m6A WERs with binding evidence from RIP-seq analysis

First, RIP-seq data underwent initial quality control and filtering with fastp [20], followed by read mapping using BWA [23]. Then, Circm6A [24] was used to identify circRNAs regulated by m6A WERS with binding evidence from the mapped RIP-seq reads.Circm6A calculates read coverages around the backsplice junction (BSJ) sites in both immunoprecipitated (IP) and INPUT samples. Differences in read coverage near BSJ sites were analyzed with Fisher's exact test, and p values were adjusted via the Benjamini—Hochberg method to identify regions with significant enrichment. CircRNAs exhibiting significantly higher read coverage around BSJ sites in IP samples compared to INPUT samples were considered to be enriched by WER antibodies. Finally, the candidate circRNAs that were also identified by CIRI2 and CIRCexplorer2 results, or were recorded in circRNA databases were retained for further analysis.

2.4. Derivation of potential m6A-modified circRNAs from m6A-seq data

We obtained m6A-modified circRNAs from m6A-seq data using the following pipeline. First, m6A-seq data underwent initial quality control and filtering with fastp [20], followed by read mapping using BWA [23]. Second, Circm6A [24] was applied to identify m6A-modified circRNAs. Circm6A calculates read coverages around the backsplice junction (BSJ) sites in both immunoprecipitated (IP) and INPUT samples. Differences in read coverage near BSJ sites were analyzed with Fisher's exact test, and p values were adjusted via the Benjamini—Hochberg method to identify regions with significant enrichment. CircRNAs exhibiting significantly higher read coverage around BSJ sites in IP samples compared to INPUT samples were considered to contain m6A sites. Finally, the candidate m6A-modified circRNAs that were also identified by CIRI2 and CIRCexplorer2 results, or were recorded in circRNA databases were retained for further analysis.

To assess the level of m6A modification of circRNAs, the RPM value of the circRNA in the immunoprecipitated (IP) sample sequenced by MeRIP was divided by the RPM value of the same circRNA in the input sample. This ratio was then used to represent the relative M6A level of each circRNA, with higher values indicating greater enrichment of the m6A modification in the circRNA fraction.

2.5. Annotation of m6A-circRNA associations

Pertinent information concerning circRNAs and their host genes, such as gene symbols, gene IDs, gene types and transcript IDs, was preferentially extracted from ENSEMBL annotation files (human: GRCh38.v90, mouse: GRCm38.v94). Experimental details and sample information were gleaned from the source literature or relevant datasets. Integrated CLIP-Seq data were downloaded from POSTAR2 [27], encompassing 220 protein-binding sites for RBPs, to identify potential RBP-binding events in circRNAs. Experimentally verified internal ribosome entry sites from the IRESbase [28] were mapped to circRNAs. The open reading frame (ORF) and miRNA sites were sourced from CSCD2.0 [29] and mapped to circRNAs. Associations between circRNAs and diseases supported by experimental evidence were gathered from resources such as circad [30], CircR2Disease [31], CircR2Disease v2.0 [32] and circRNADisease v2.0 [33], offering new insights into disease pathogenesis from the perspective of m6A-circRNA associations. To standardize the results, including the gene symbols, the genomic coordinates from all the data sources were converted to hg38 or mm10 values using the LiftOver program [34].

2.6. Statistical analysis

All the statistical analyses were conducted using R (version 4.3.1), with data visualization performed using the ggplot2 package (version 3.5.1). The following statistical methods were employed: the Wilcoxon rank-sum test, a nonparametric test, was used to compare the difference in circRNA length, circRNA expression, and exon length between groups; differences in circRNA annotation proportions were evaluated using chi-square test. Significance levels (e.g., $p < 0.05$, $^{*}p < 0.01$, $^{**}p < 0.001$, $^{***}p < 0.0001$) are displayed directly on the graphs.

2.7. Database and web interface implementation

MySQL was employed for data storage and management within the m6A2Circ database. The server-backend development was executed using the Flask framework in Python, and the web-frontend interfaces were constructed using the Hyper Text Markup Language (HTML), Cascading Style Sheets (CSS) and JavaScript (JS). All the interactive diagrams were generated by ECharts to visualize the analysis results.

2.8. Cell lines and cell culture

The human esophageal squamous carcinoma KYSE30 cells were purchased from BNCC (Beijing, China) and cultured in RPMI-1640 medium (Procell) containing 10 % fetal bovine serum (Procell). The cells were grown in a 5 % CO2 humidified incubator at 37 °C.

2.9. RNA extraction and purification

Total RNA was extracted from KYSE30 cells via TRIzol reagent (Invitrogen) and chloroform. After mixing thoroughly, the mixture was kept on ice for 10 min and centrifuged for 15 min at 12,000 × rpm at 4 °C. The upper phase was transferred to sterile and RNase-free tubes, and an equal volume of isopropanol was added for RNA precipitation for 10 min at room temperature, followed by centrifugation for 10 min at 12,000 × rpm at 4 °C. After the supernatant was discarded, the precipitate was rinsed with 75 % ethanol and centrifuged for 5 min at 12,000 × rpm at 4 °C. Finally, the supernatant was discarded, and the pellet was left to air dry for 5–10 min. When the appearance changed from a milky white pellet to a slightly translucent pellet, the RNA was dissolved in 50 μl of RNase-free water. The RNA concentration and purity were measured at OD260 and OD280.

2.10. Quantitative real-time PCR (qRT—PCR) analysis

The circRNAs and mRNAs were reverse transcribed in a volume of 20 μl with a HiScript II 1st Strand cDNA Synthesis Kit (Vazyme) using random hexamers with or without oligo(dT) $_{23}$VN. Real-time quantification was performed by a CFX96 system (Bio-Rad) and an AceQ qPCR SYBR Green Master Mix kit (Vazyme), with GADPH used as an internal reference. Relative expression was calculated using the $2^{-\Delta\Delta Ct}$ method. The sequences of primers used are listed in Supplementary Table S3. The data are expressed as the means ± standard deviations (SDs), with n = 3. Statistical comparisons were performed using Student's t test. Significance levels are indicated as follows: * for $P < 0.05$, * * for $P < 0.01$, and * ** for $P < 0.001$.

2.11. RNase R treatment assay

Four micrograms of total RNA was digested with 1 μl of RNas R (20

units/μl, Biosearch Technologies, RNR07250) in a total reaction volume of 20 μl at 37 °C for 30 min. The enzyme was inactivated at 70 °C for 10 min. For controls, RNas R was replaced with ddH2O. Afterward, 4 μl of the reactants were directly used as templates in the RT—qPCRs as described. The PCR products were subjected to 2 % agarose gel electrophoresis.

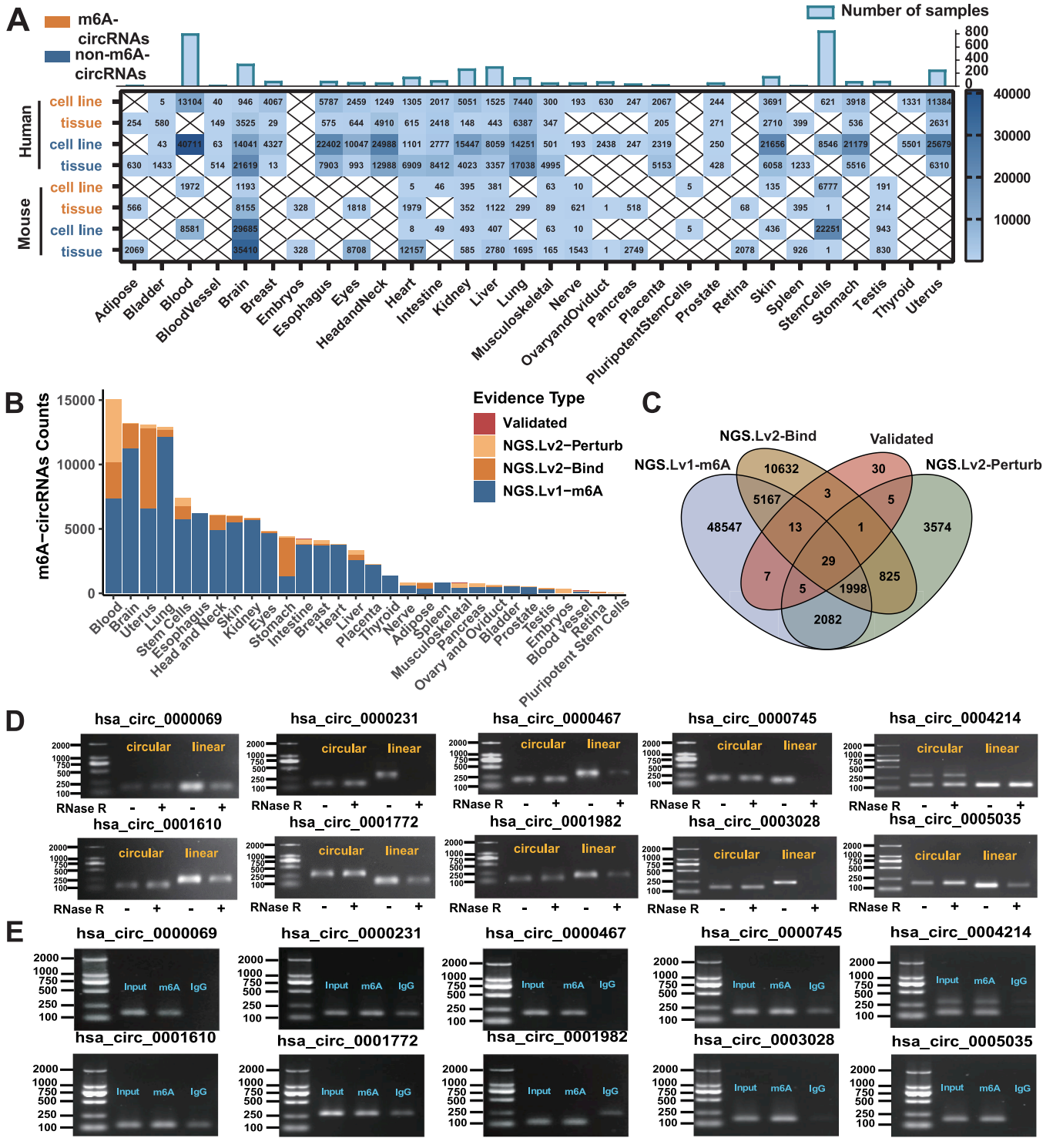

Fig. 2. Overview of m6A-circRNA associations in m6A2Circ. (A) A table displaying the number of m6A-circRNA associations and non-m6A-circRNAs within m6A2Circ, categorized by various tissue types. The bars at the top of the table indicate the number of high-throughput sequencing samples from different tissues. (B) A stacked column chart illustrating m6A-circRNAs in m6A2Circ across different tissue types, classified into four confidence levels. If an m6A-circRNA is associated with multiple confidence levels, it is represented multiple times in the chart, with each confidence level assigned a distinct color. (C) Overlap between records with different types of evidence for the same m6A-circRNA. (D) Validation of 10 candidate m6A-circRNAs via qRT—PCR and RNase R treatment in KYSE30 cells. (E) Validation of the m6A modification of 10 m6A-circRNAs using MeRIP-qPCR after RNase R treatment in KYSE30 cells. The data in E and F are the means ± SDs (n = 3). * , $P < 0.05$; * *, $P < 0.01$; * ** , and $P < 0.001$ for Student's t test compared with each control.

2.12. Methylated RNA immunoprecipitation qPCR (MeRIP-qPCR)

MeRIP-qPCR was conducted using the riboMeRIP™ m6A Transcript Profiling Kit (RiboBio, China) according to the manufacturer's protocol without fragmentation. Briefly, 1/10 of the 50 μg of purified total RNA was collected and stored in a −80 °C freezer as the input. The remaining proteins were immunoprecipitated with 5 μg of m6A-specific antibody, which was linked to magnetic beads A/G. Mouse IgG (eBioscience™, Invitrogen) was used as the control. Then, the immunopurified RNA was purified using the Hipure Serum/plasma miRNA Midi Kit (Magen, R4317–01). The RNAs from the input, IgG and m6A-specific antibody IP samples were used for further analysis by RT—qPCR according to the procedure described above.

3. Results

3.1. Database content

Currently, m6A2Circ encompasses 198,804 m6A-circRNA associations covering 4300 samples from 30 tissue types in humans and mice (Fig. 2A, B). These m6A-circRNA associations are cataloged into four evidence types: (i) 'Validated': 253 and 14 m6A-circRNA associations for humans and mice, respectively, were validated by in vivo or in vitro experiments such as MeRIP-qPCR, RNA pull-down, RIP, RT—qPCR, and Western blot; (ii) 'NGS. Lv1-m6A': A total of 115,539 and 43,081 m6A-circRNA associations were identified from MeRIP-seq data for humans and mice, respectively; (iii) 'NGS. Lv2-Perturb': 8703 and 1548 m6A-circRNA associations were inferred from RNA-seq data of samples subjected to WER perturbation for humans and mice, respectively; (iv) 'NGS. Lv2-Bind': 24,641 and 5025 m6A-circRNA associations with binding evidence were inferred from RIP-seq data for humans and mice,

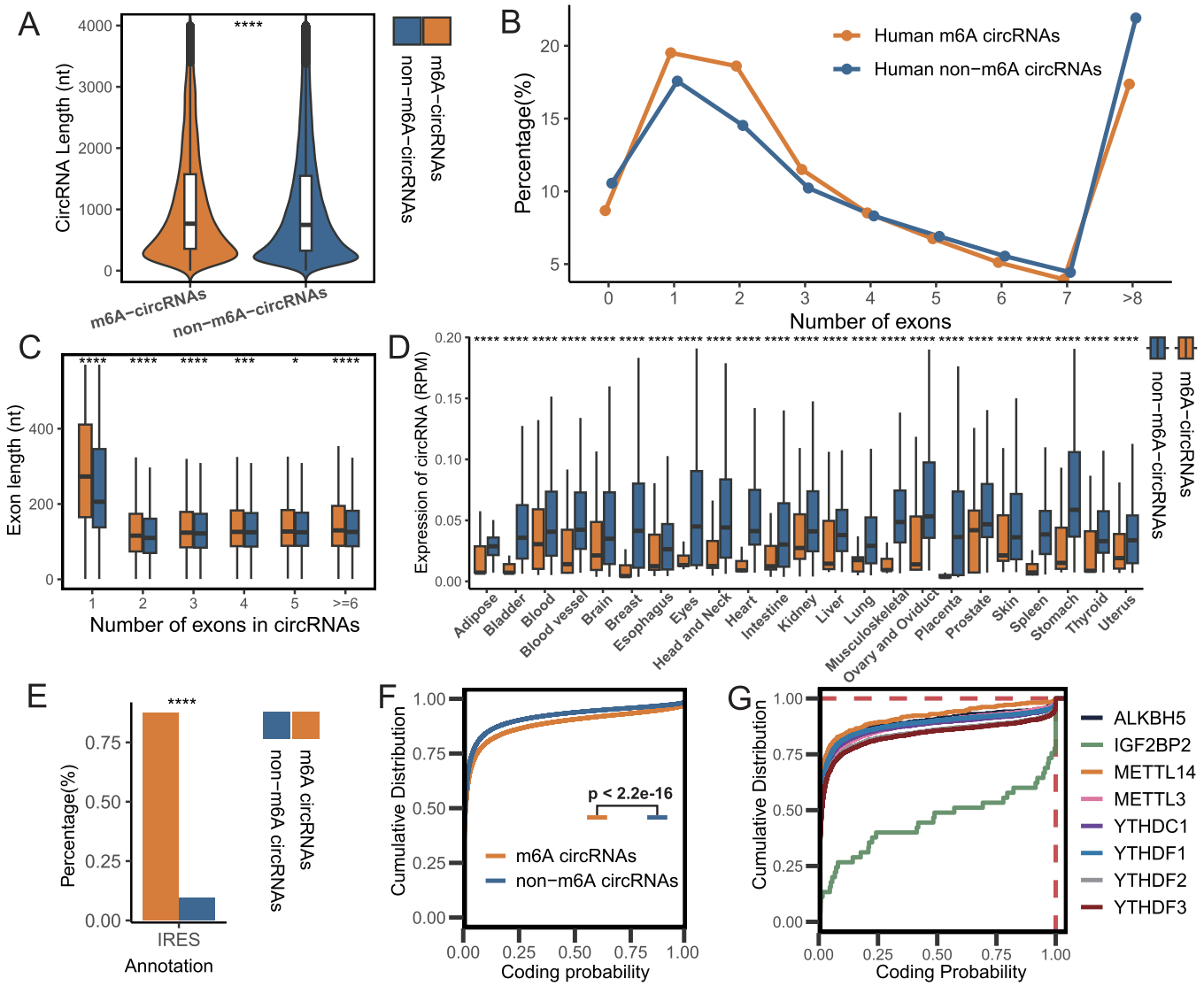

Fig. 3. Characterization of m6A-circRNAs in humans. (A) Violin plot of the lengths of m6A-circRNAs and non-m6A-circRNAs in human circRNAs. (B) The percentage of circRNAs (y-axis) was calculated on the basis of the number of exons that each circRNA spans (x-axis) for m6A-circRNAs and non-m6A-circRNAs in humans. (C) Exon lengths of m6A-circRNAs and non-m6A-circRNAs spanning different numbers of exons in humans. The distributions of exon length (y-axis) for input m6A-circRNAs and non-m6A-circRNAs are plotted on the basis of the number of exons spanned by each circRNA (x-axis). (D) Boxplot of the differential expression of m6A-circRNAs and non-m6A-circRNAs in different tissue types in humans. (E) Differences in the annotation shares of human m6A-circRNAs and non-m6A-circRNAs in m6A2Circ (IRES: internal ribosome entry site). (F) Cumulative fraction of coding probability scores predicted by CPAT for m6A- and non-m6A-circRNAs in humans. (G) Cumulative fraction coding probability scores predicted by the CPAT for m6A-circRNAs of specific WERs in humans. Statistical tests: Wilcoxon test for A, C, D; chi-square test for E. (* $P < 0.05$, ** $P < 0.01$, *** $P < 0.001$, **** $P < 0.0001$).

respectively (Fig. 2B). Notably, 62.37 % of the validated m6A-circRNA associations were also detected by other evidence types, highlighting the reliability of the associations cataloged in m6A2Circ (Fig. 2C). Next, we selected 10 m6A-circRNA associations supported by NGS. Lv1-m6A evidence for experimental validation. Compared with their corresponding linear RNAs, all 10 candidates exhibited resistance to RNase R treatment, as demonstrated by RT—PCR (Fig. 2D). The junction sequences of these 10 candidates were confirmed via Sanger sequencing (Fig. S1A). Further verification of m6A modification in these circRNAs was conducted via MeRIP—qPCR following RNase R treatment. All 10 candidates were confirmed to be m6A-modified, as indicated by significant enrichment differences between the m6A MeRIP and IgG groups (Fig. 2E, Fig. S1B). These results reinforce the credibility of the m6A-circRNA associations documented in m6A2Circ.

3.2. Characterization of m6A-modified circRNAs

We conducted a comparative analysis between m6A-modified circRNAs (m6A-circRNAs) and non-m6A-modified circRNAs (non-m6A-circRNAs) to investigate the characteristics of m6A-modified circRNAs. CircRNAs identified through three high-throughput sequencing methods that lacked evidence of m6A-circRNA associations in any sample were classified as nonm6A-circRNAs. Our analysis revealed that m6A-circRNAs were longer in both humans (Fig. 3A) and mice (Fig. S2A). Additionally, m6A-circRNAs had fewer exons than non-m6A-circRNAs did (Fig. 3B and Fig. S2B), while the exon lengths of m6A-circRNAs were generally longer than those of non-m6A-circRNAs were (Fig. 3C and Fig. S2C). These findings suggest that m6A methylation tends to occur preferentially in circRNAs derived from long single exons, which aligns with previous observations [35].

We observed that the expression levels of m6A-circRNAs were lower than those of non-m6A-circRNAs across all tissue types (Fig. 3D and Fig. S2D). These findings suggest that m6A may play a significant role in regulating circRNA expression. Additionally, m6A-circRNAs presented a greater percentage of IRES annotations than non-m6A-circRNAs in humans (Fig. 3E), indicating that m6A-circRNAs are more likely to be translated. Using the coding potential assessment tool (CPAT) [36], we found that m6A-circRNAs had significantly higher coding probability

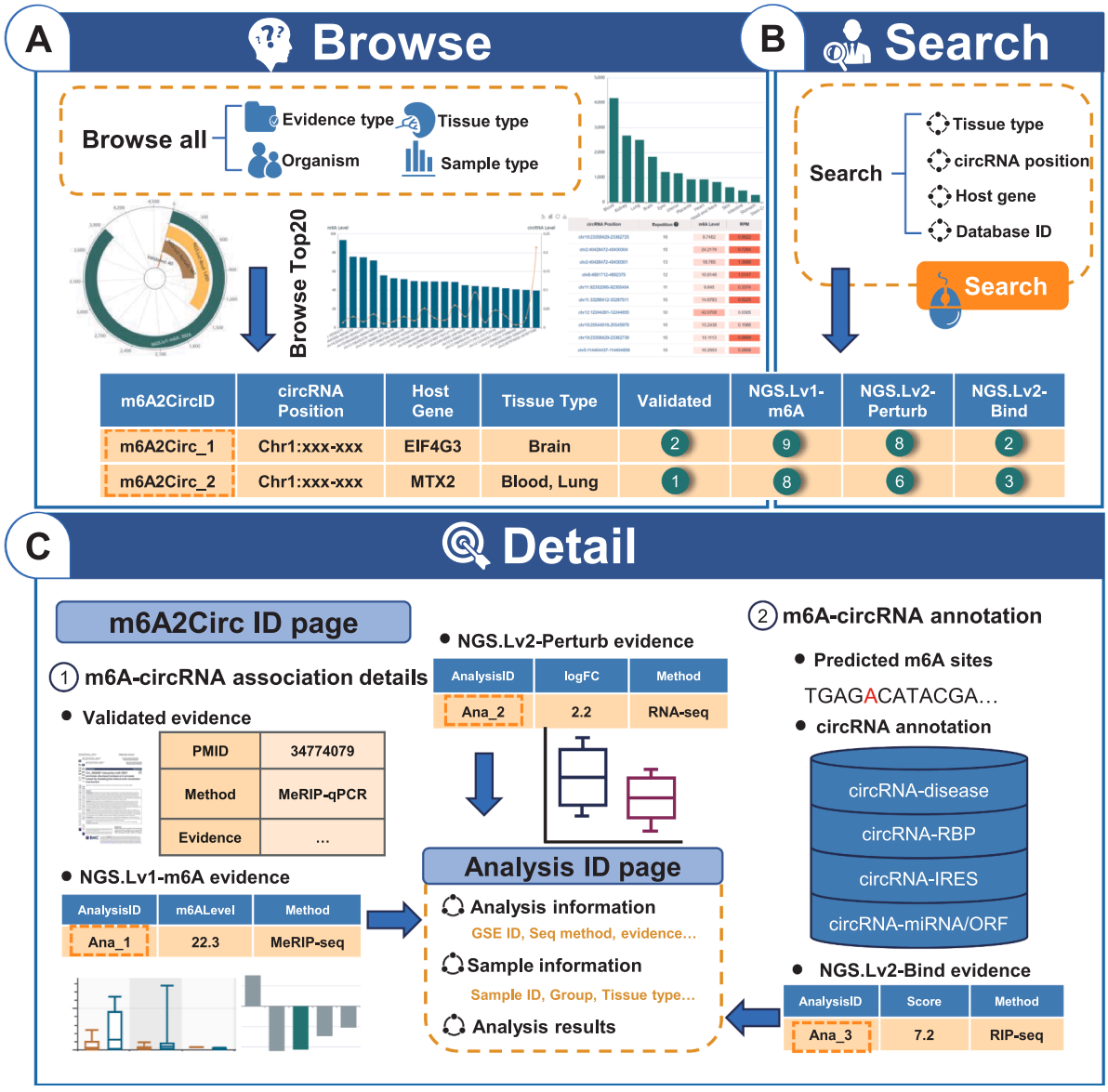

Fig. 4. Introduction of the m6A2Circ web interface. (A) The browsing interface of m6A2Circ. (B) The main modules of the search interface in m6A2Circ. (C) Detailed information about m6A-circRNA associations can be accessed by clicking on the m6A2Circ ID. Clicking on the analysis ID on the m6A2Circ ID page links to more details about the specific analysis.

scores than non-m6A-circRNAs ($P < 2.2e{-}16$, Kolmogorov—Smirnov test) (Figs. 3F and S2E). Furthermore, m6A-circRNA associations were integrated with NGS. Lv2-Bind evidence revealed that circRNAs bound by IGF2BP2 and YTHDF3 presented the highest coding probability scores in humans and mice, respectively. These findings suggest that these two m6A readers may increase the translation of m6A-circRNAs (Figs. 3G and S2F).

3.3. Web interface and usage

m6A2Circ provides a user-friendly web interface that enables users to explore m6A-circRNA associations quickly and interactively (Fig. 4). On the browse page (Fig. 4A), users can explore m6A-circRNA associations by tissue type, organism, sample type, and evidence type of interest. Advanced filtering functions in the browse table allow users to refine their queries by combining multiple conditions. Upon selection, visual representations, such as polar and bar plots, illustrate the distribution of m6A-circRNAs across four confidence levels and various tissue types. Simultaneously, the browsing table displays the m6A-circRNA associations that match the user's selections. To assist users in filtering out noise, the browse table includes counts for validated evidence, NGS. Lv1-m6A, NGS.Lv2-Perturb, and NGS.Lv2-Bind. To help identify m6A-circRNAs worthy of further investigation in different tissues, m6A2Circ offers a Top20 page. By selecting a species and tissue of interest, users can view a bar-line chart representing the top 20 circRNAs with the highest m6A modification levels alongside their expression levels in that tissue. Additionally, a table lists these 20 circRNAs on the basis of the number of repeats across four confidence levels, along with their expression and m6A levels. On the search page (Fig. 4B), users can search for m6A-circRNA associations using criteria such as organism, tissue type, host gene, circRNA position, genomic region of circRNA position, m6A2Circ ID, and circRNA ID from other databases.

When clicking on an m6A2Circ ID in either the browse or search result table, users are directed to a detail page containing comprehensive information about the m6A-circRNA association. This detail page presents various types of evidence, including 'Validated', 'NGS. Lv1', and 'NGS.Lv2' (Fig. 4C). In the 'Validated Evidence' section, users can find literature sources, cell line/tissue information, experimental methods, motif sequences, affected biological processes, and descriptions of the evidence. The 'Perturbation Evidence' section contains WER information, sample details, differential analysis results (including logFC and p value), sequencing methods, dataset links, and the direction of WER perturbation, along with box plot visualizations of circRNA expression levels. Similarly, the 'Binding Evidence' section provides WER information, sample data, analysis results (including enrichment scores and FDR), sequencing methods, and dataset links. Additionally, m6A2Circ offers multiple annotations for circRNAs, including predicted m6A sites, mature sequences, related diseases, RBPs, and IRES, miRNA, and ORF annotations. Users can click on the analysis ID on the detail page to access further dataset information, such as analysis tools, sample details, and comprehensive analysis results.

M6A2Circ also allows users to download all validated and potential m6A-circRNAs from both human and mouse samples. Detailed guidance on the use of m6A2Circ can be found on the 'Help' page.

4. Summary and perspectives

Identifying the associations between m6A modifications and circRNAs is crucial for elucidating the molecular mechanisms that regulate circRNAs and for exploring their potential applications. To our knowledge, m6A2Circ is the first comprehensive database specifically focused on the m6A modification of circRNAs in humans and mice. In contrast to existing databases, such as RNA modification resources (e.g., RMVar [37], Rmbase [38], MODOMICS [39], and RNAMDB [40]), which primarily collect and annotate RNA modification sites in linear genes, and circRNA databases (e.g., circBase [17], circAtlas 3.0 [18], CIRCpedia v2 [19], circRNADisease v2.0 [33], and CSCD2.0 [29]), which focus mainly on circRNA collection and annotation, m6A2Circ uniquely catalogs regulatory associations between m6A modifications and circRNAs. This resource provides insights into how m6A modifications influence circRNA functions and aids in understanding disease mechanisms, biomarker discovery, and therapeutic targeting specific to m6A-modified circRNAs.

However, m6A2Circ has limitations. First, it currently includes data from only two commonly studied organisms: humans and mice. Second, most of the m6A-circRNAs in the database are derived from short-read sequencing data, which do not incorporate long-read sequencing technologies—an emerging trend in the detection of modifications and circRNAs. Third, as Circm6A can detects only the m6A sites near the back-splicing junction, the circRNAs with m6A sites locating distal to junction sites will not be included in the current database. We aim to address these limitations in future updates of m6A2Circ.

In summary, we believe that m6A2Circ, as a pioneering portal for compiling m6A-modified circRNAs, will significantly benefit the research community and facilitate novel discoveries regarding the interplay between m6A and circRNAs. As a long-term goal, we plan to continue updating m6A2Circ to increase its utility and comprehensiveness. To further expanding the scope of the database and its application in RNA modification research, in the future updates we will include the integration of other RNA modifications detected by sequencing technologies, such as m7G, m1A, m5C, and m5U.

Funding

This study was supported by the Guangdong Basic and Applied Basic Research Foundation [2021B1515020108].

CRediT authorship contribution statement

Wang Li: Writing – review & editing, Investigation. **Yang Rui:** Supervision, Investigation, Data curation. **Huang Yuantai:** Writing – review & editing, Supervision. **Bao Xiaoqiong:** Software, Investigation. **Gao Shegan:** Writing – review & editing, Supervision, Project administration. **Zuo Zhixiang:** Writing – review & editing, Funding acquisition, Conceptualization. **Yang Haibo:** Visualization, Methodology. **Yang Qingtao:** Visualization, Data curation. **He Li-Na:** Methodology, Data curation. **Ma Lixia:** Visualization, Methodology. **Gu Bianli:** Validation, Methodology, Formal analysis. **Li Yongtian:** Writing – original draft, Software, Methodology, Formal analysis, Data curation. **Chen Ke:** Writing – review & editing, Supervision, Project administration. **Zhao Xueya:** Writing – review & editing, Supervision, Conceptualization.

Declaration of Competing Interest

The authors declare that the research was conducted in the absence of any commercial or financial relationships that could be construed as a potential conflict of interest.

Acknowledgments

The authors would like to acknowledge the Supercomputing Center of Chongqing Medical University for providing the computational resources used in this study.

Appendix A. Supporting information

Supplementary data associated with this article can be found in the online version at doi:10.1016/j.csbj.2025.02.018.

Availability of data

M6A2Circ is a comprehensive online database available at

http://m6a2circ.canceromics.org/.

References

[1] Xu H, Guo S, Li W, Yu P. The circular RNA Cdr1as, via miR-7 and its targets, regulates insulin transcription and secretion in islet cells. Sci Rep 2015;5:12453.
[2] Liu CX, Li X, Nan F, Jiang S, Gao X, Guo SK, Xue W, Cui Y, Dong K, Ding H, et al. Structure and Degradation of Circular RNAs Regulate PKR Activation in Innate Immunity. Cell 2019;177:865–80. e821.
[3] Zhang M, Zhao K, Xu X, Yang Y, Yan S, Wei P, Liu H, Xu J, Xiao F, Zhou H, et al. A peptide encoded by circular form of LINC-PINT suppresses oncogenic transcriptional elongation in glioblastoma. Nat Commun 2018;9:4475.
[4] Xu X, Zhang J, Tian Y, Gao Y, Dong X, Chen W, Yuan X, Yin W, Xu J, Chen K, et al. CircRNA inhibits DNA damage repair by interacting with host gene. Mol Cancer 2020;19:128.
[5] Chen S, Cao X, Zhang J, Wu W, Zhang B, Zhao F. circVAMP3 Drives CAPRIN1 Phase Separation and Inhibits Hepatocellular Carcinoma by Suppressing c-Myc Translation. Adv Sci (Weinh) 2022;9:e2103817.
[6] Su Y, Lv X, Yin W, Zhou L, Hu Y, Zhou A, Qi F. CircRNA Cdr1as functions as a competitive endogenous RNA to promote hepatocellular carcinoma progression. Aging (Albany NY) 2019;11:8183–203.
[7] Song M, Zhao G, Sun H, Yao S, Zhou Z, Jiang P, Wu Q, Zhu H, Wang H, Dai C. circPTPN12/miR-21–5 p/Δ Np63 α pathway contributes to human endometrial fibrosis. Elife 2021;10:e65735.
[8] Wu WP, Pan YH, Cai MY, Cen JM, Chen C, Zheng L, Liu X, Xiong XD. Plasma-Derived Exosomal Circular RNA hsa_circ_0005540 as a Novel Diagnostic Biomarker for Coronary Artery Disease. Dis Markers 2020;2020:3178642.
[9] Akhter R. Circular RNA and Alzheimer's Disease. Adv Exp Med Biol 2018;1087: 239–43.
[10] Zhang C, Han X, Yang L, Fu J, Sun C, Huang S, Xiao W, Gao Y, Liang Q, Wang X, et al. Circular RNA circPPM1F modulates M1 macrophage activation and pancreatic islet inflammation in type 1 diabetes mellitus. Theranostics 2020;10: 10908–24.
[11] Yang Y, Fan X, Mao M, Song X, Wu P, Zhang Y, Jin Y, Yang Y, Chen L-L, Wang Y, et al. Extensive translation of circular RNAs driven by N6-methyladenosine. Cell Res 2017;27:626–41.
[12] Park OH, Ha H, Lee Y, Boo SH, Kwon DH, Song HK, Kim YK. Endoribonucleolytic Cleavage of m(6)A-Containing RNAs by RNase P/MRP Complex. Mol Cell 2019;74: 494–507. e498.
[13] Ries RJ, Zaccara S, Klein P, Olarerin-George A, Namkoong S, Pickering BF, Patil DP, Kwak H, Lee JH, Jaffrey SR. m(6)A enhances the phase separation potential of mRNA. Nature 2019;571:424–8.
[14] Chen RX, Chen X, Xia LP, Zhang JX, Pan ZZ, Ma XD, Han K, Chen JW, Judde JG, Deas O, et al. N(6)-methyladenosine modification of circNSUN2 facilitates cytoplasmic export and stabilizes HMGA2 to promote colorectal liver metastasis. Nat Commun 2019;10:4695.
[15] Zhao J, Lee EE, Kim J, Yang R, Chamseddin B, Ni C, Gusho E, Xie Y, Chiang CM, Buszczak M, et al. Transforming activity of an oncoprotein-encoding circular RNA from human papillomavirus. Nat Commun 2019;10:2300.
[16] Zhang X, Xu Y, Qian Z, Zheng W, Wu Q, Chen Y, Zhu G, Liu Y, Bian Z, Xu W, et al. circRNA_104075 stimulates YAP-dependent tumorigenesis through the regulation of HNF4a and may serve as a diagnostic marker in hepatocellular carcinoma. Cell Death Dis 2018;9:1091.
[17] Glažar, P., Papavasileiou, P. and Rajewsky, N. circBase: a database for circular RNAs. *RNA (New York, N.Y.)*, 20, 1666-1670.
[18] Wu W, Zhao F, Zhang J. circAtlas 3.0: a gateway to 3 million curated vertebrate circular RNAs based on a standardized nomenclature scheme. Nucleic Acids Res 2024;52. D52-D60.
[19] Dong R, Ma XK, Li GW, Yang L. CIRCpedia v2: An Updated Database for Comprehensive Circular RNA Annotation and Expression Comparison. Genom Proteom Bioinforma 2018;16:226–33.
[20] Chen, S., Zhou, Y., Chen, Y. and Gu, J. fastp: an ultra-fast all-in-one FASTQ preprocessor. *Bioinformatics*, **34**, i884-i890.
[21] Gao Y, Zhang J, Zhao F. Circular RNA identification based on multiple seed matching. Brief Bioinform 2018;19:803–10.
[22] Zhang XO, Dong R, Zhang Y, Zhang JL, Luo Z, Zhang J, Chen LL, Yang L. Diverse alternative back-splicing and alternative splicing landscape of circular RNAs. Genome Res 2016;26:1277–87.
[23] Li, H. and Durbin, R. Fast and accurate short read alignment with Burrows-Wheeler transform. *Bioinformatics*, **25**, 1754-1760.
[24] Ye Y, Feng W, Zhang J, Zhu K, Huang X, Pan L, Su J, Zheng Y, Li R, Deng S, et al. Genome-wide identification and characterization of circular RNA m(6)A modification in pancreatic cancer. Genome Med 2021;13:183.
[25] Zhang J, Chen S, Yang J, Zhao F. Accurate quantification of circular RNAs identifies extensive circular isoform switching events. Nat Commun 2020;11:90.
[26] Robinson, M.D., McCarthy, D.J. and Smyth, G.K. edgeR: a Bioconductor package for differential expression analysis of digital gene expression data. *Bioinformatics*, **26**, 139-140.
[27] Zhu, Y., Xu, G., Yang, Y.T., Xu, Z., Chen, X., Shi, B., Xie, D., Lu, Z.J. and Wang, P. POSTAR2: deciphering the post-transcriptional regulatory logics. *Nucleic acids research*, **47**, D203-D211.
[28] Zhao J, Li Y, Wang C, Zhang H, Zhang H, Jiang B, Guo X, Song X. IRESbase: a comprehensive database of experimentally validated internal ribosome entry sites. Genom Proteom Bioinforma 2020;18:129–39.
[29] Feng J, Chen W, Dong X, Wang J, Mei X, Deng J, Yang S, Zhuo C, Huang X, Shao L, et al. CSCD2: an integrated interactional database of cancer-specific circular RNAs. Nucleic Acids Res 2022;50:D1179–83.
[30] Rophina M, Sharma D, Poojary M, Scaria V. Circad: a comprehensive manually curated resource of circular RNA asso ciated with diseases. Database (Oxf) 2020: baaa019.
[31] Fan C, Lei X, Fang Z, Jiang Q, Wu F-X. CircR2Disease: a manually curated database for experimentally supporte d circular RNAs associated with various diseases. Database (Oxf) 2018. bay044.
[32] Fan C, Lei X, Tie J, Zhang Y, Wu FX, Pan Y. CircR2Disease v2.0: An Updated Web Server for Experimentally Validated circRNA-disease Associations and Its Application. Genom Proteom Bioinforma 2022;20:435–45.
[33] Sun ZY, Yang CL, Huang LJ, Mo ZC, Zhang KN, Fan WH, Wang KY, Wu F, Wang JG, Meng FL, et al. circRNADisease v2.0: an updated resource for high-quality experimentally supported circRNA-disease associations. Nucleic Acids Res 2024; 52. D1193-D1200.
[34] Nassar, L.R., Barber, G.P., Benet-Pagès, A., Casper, J., Clawson, H., Diekhans, M., Fischer, C., Gonzalez, J.N., Hinrichs, A.S., Lee, B.T. *et al.* The UCSC Genome Browser database: 2023 update. *Nucleic acids research*, **51**, D1188-D1195.
[35] Zhou C, Molinie B, Daneshvar K, Pondick JV, Wang J, Van Wittenberghe N, Xing Y, Giallourakis CC, Mullen AC. Genome-Wide Maps of m6A circRNAs Identify Widespread and Cell-Type-Specific Methylation Patterns that Are Distinct from mRNAs. Cell Rep 2017;20:2262–76.
[36] Wang L, Park HJ, Dasari S, Wang S, Kocher JP, Li W. CPAT: Coding-Potential Assessment Tool using an alignment-free logistic regression model. Nucleic Acids Res 2013;41:e74.
[37] Luo X, Li H, Liang J, Zhao Q, Xie Y, Ren J, Zuo Z. RMVar: an updated database of functional variants involved in RNA modifications. Nucleic Acids Res 2021;49: D1405–12.
[38] Xuan J, Chen L, Chen Z, Pang J, Huang J, Lin J, Zheng L, Li B, Qu L, Yang J. RMBase v3.0: decode the landscape, mechanisms and functions of RNA modifications. Nucleic Acids Res 2024;52. D273-D284.
[39] Boccaletto P, Stefaniak F, Ray A, Cappannini A, Mukherjee S, Purta E, Kurkowska M, Shirvanizadeh N, Destefanis E, Groza P, et al. MODOMICS: a database of RNA modification pathways. 2021 update. Nucleic Acids Res 2022;50. D231-D235.
[40] Cantara WA, Crain PF, Rozenski J, McCloskey JA, Harris KA, Zhang X, Vendeix FA, Fabris D, Agris PF. The RNA Modification Database, RNAMDB: 2011 update. Nucleic Acids Res 2011;39:D195–201.